

Theory of Fano Resonances in Graphene: The Kondo effect probed by STM

T. O. Wehling,^{1,*} H. P. Dahal,² A. I. Lichtenstein,¹ M. I. Katsnelson,³ H. Manoharan,⁴ and A. V. Balatsky^{2,5,†}

¹*Institut für Theoretische Physik I, Universität Hamburg, D-20355 Hamburg, Germany*

²*Theoretical Division, Los Alamos National Laboratory, Los Alamos, New Mexico 87545, USA*

³*Institute for Molecules and Materials, Radboud University Nijmegen, NL-6525 AJ Nijmegen, The Netherlands*

⁴*Department of Physics, Stanford Institute for Materials and Energy Science, Stanford University, Stanford, CA 94305 USA*

⁵*Center for Integrated Nanotechnologies, Los Alamos National Laboratory, Los Alamos, New Mexico 87545, USA*

(Dated: November 9, 2018)

We consider the theory of Kondo effect and Fano factor energy dependence for magnetic impurity (Co) on graphene. We have performed a first principles calculation and find that the two dimensional E_1 representation made of d_{xz}, d_{yz} orbitals is likely to be responsible for the hybridization and ultimately Kondo screening for cobalt on graphene. There are few high symmetry sites where magnetic impurity atom can be adsorbed. For the case of Co atom in the middle of hexagon of carbon lattice we find anomalously large Fano q -factor, $q \approx 80$ and strongly suppressed coupling to conduction band. This anomaly is a striking example of quantum mechanical interference related to the Berry phase inherent to graphene band structure.

PACS numbers:

Scanning tunneling microscopy (STM) allows us to probe the electronic properties of conducting materials with atomic scale spacial resolution. This experimental technique is particularly well suited to study electron-correlation phenomena. One of the most famous correlation phenomena is the Kondo effect arising from a localized magnetic moment being screened by the conduction electrons¹. It results in a sharp Abrikosov-Suhl resonance in local density of states (LDOS) of the impurity at the Fermi level and below a characteristic Kondo temperature, T_K . While the Kondo effect is well understood for impurities in bulk materials and simple model systems, STM has been substantial for revealing the intricacies of Kondo effect at conventional metal surfaces. One well known example is the Kondo effect caused by Co ad-atoms on a Cu (111) surface²: It shows that the rich electronic structure of three-dimensional metals like Cu, in general, makes impurity effects at their surfaces³⁻⁵ depending strongly on atomistic details and requires to understand interaction mechanisms in detail.

Graphene - a monolayer of carbon atoms arranged in a honeycomb lattice - is the first truly two dimensional material⁶ and provides a two-dimensional electron gas with distinct and highly symmetric low energy electronic structure: At two non-equivalent corners of the Brillouin zone, K and K', the linearly dispersing valence and conduction band touch forming a conical point and leading to the Berry phase π ^{7,8}. Thus, electronic excitations in graphene resemble massless Dirac fermions with the speed of light being replaced by the Fermi velocity $v_f \approx c/300$. Therefore, graphene provides an important model system for understanding quantum effects in reduced dimensions and in presence of an "ultra-relativistic" conduction electron bath.

A theoretical study showed that even in undoped graphene the Kondo effect can exist above a certain critical coupling despite the linearly vanishing density of states⁹⁻¹¹, a situation very similar to magnetic impurities

in the pseudogap phase of high T_c superconductors^{9,12}. Moreover, back-gating⁶ as well as chemical doping^{13,14} allows one to control the chemical potential in graphene and to tune Kondo physics and electron tunneling in this way.

In this paper, we address how the Kondo effect manifests in STM experiments on graphene and why Fano resonances in the STM spectra can depend unusually strong on the chemical potential as well as the real space position of the impurity. To this end, we firstly consider the single impurity Anderson model with graphene providing the host electronic structure and compare to simple model of usual metal surface. With this background, we turn to a more realistic ab-initio based description of magnetic impurities on graphene and discuss the case of Co ad-atoms as in the recent experiment by Manoharan et al.¹⁵. By comparison to Co on Cu (111), an extensively studied system³⁻⁵ possessing also hexagonal symmetry of the surface, demonstrate the particular importance of impurity induced resonances in graphene. Furthermore, we analyze impurities being bound to different sites of the graphene lattice and show that there one can expect a strong adsorption site dependence of Fano factors in STM experiments.

Model for electron tunneling close to impurities. The π -band the tight-binding Hamiltonian of graphene reads as¹⁶

$$\hat{H}_0 = -t \sum_{\langle i,j \rangle} \left(a_i^\dagger b_j + b_j^\dagger a_i \right), \quad (1)$$

where a_i and b_i are the Fermi operators of electrons in the carbon p_z orbital of sublattice atoms A and B in the cell at R_i , respectively. The sum includes all pairs of nearest-neighbor carbon atoms and $t \approx 2.7$ eV is the hopping parameter. With the Fourier transformed operators a_k (b_k), defined by $a_i = \int_{\Omega_B} \frac{d^2k}{\Omega_B} e^{ikR_i} a_k$ and b_i analogously,

the Hamiltonian can be rewritten as

$$\hat{H}_0 = \int_{\Omega_B} \frac{d^2k}{\Omega_B} \Psi_k^\dagger H_k \Psi_k \text{ with } \Psi(k) = \begin{bmatrix} a_k \\ b_k \end{bmatrix}, \quad (2)$$

H_k is the k -dependent 2×2 matrix

$$H_k = \begin{pmatrix} 0 & \xi(k) \\ \xi^*(k) & 0 \end{pmatrix}, \quad (3)$$

with $\xi(k) = -t \sum_{j=1}^3 e^{ik(b_j - b_1)}$, b_j ($j = 1, 2, 3$) are the vectors connecting neighboring atoms¹⁷, and Ω_B is the area of the Brillouin zone. An impurity contributing a localized orbital, $\hat{H}_{\text{imp}} = \epsilon_{\text{imp}} \sum_{\sigma} d_{\sigma}^{\dagger} d_{\sigma} + U n_{\uparrow} n_{\downarrow}$, with Fermi operator d , energy ϵ_{imp} and on-site Coulomb repulsion U is considered. Its hybridizations with the graphene bands is described by, $\hat{V} = \sum_{k,\sigma} \Psi_{k,\sigma}^{\dagger} V_k d_{\sigma} + \text{h.c.}$. This problem has been extensively discussed for normal metals and is usually called ‘‘Anderson impurity model’’¹.

In this framework, the connection between a tip and a sample in the STM experiment can be expressed by the transfer Hamiltonian

$$M = \sum_{\sigma} (M_{dt} d_{\sigma}^{\dagger} t_{\sigma} + \text{H.c.}) + \sum_{\nu\sigma} (\Psi_{k\sigma}^{\dagger} M_{kt} t_{\sigma} + \text{H.c.}) \quad (4)$$

describing tunneling of electrons from and to the STM tip with the tunneling matrix elements M_{dt} and M_{kt} and the Fermi operators t_{σ} (t_{σ}^{\dagger}) for electrons in the STM tip.

The Fano q -factor in the STM dI/dV spectra can be understood in terms of this model by using the equation of motion approach from Ref. 18. One finds

$$q = \frac{A}{B} \quad (5)$$

with

$$A = M_{dt} + \sum_k M_{kt} V_k \text{P} \left(\frac{1}{E_F - \epsilon_{\nu}} \right) \quad (6)$$

and

$$B = \pi \sum_k M_{kt} V_k \delta(E_F - \epsilon_{\nu}), \quad (7)$$

where P is the principle value symbol.

To obtain qualitative insights we proceed by simplifying these expressions: For a conduction electron state k , denote its probability density integrated about an atomic sphere centered at the Co-atom by $|\Psi_k|^2$. Then, if the tip is directly above the Co impurity, one can approximate

$$M_{kt} V_{dk} = |\Psi_k|^2 M V \quad (8)$$

with MV independent of k . Thus, Eq. (6) and Eq. (7) yield

$$A = M_{dt} + M V \text{Re } G(E_F) \quad (9)$$

and

$$B = M V \text{Im } G(E_F) \quad (10)$$

with the local conduction electron Green function $G(E) = \sum_{\nu} \frac{|\Psi_k|^2}{E - \epsilon_k - i0^+}$. As argued in Ref 5, this simple model has proved successful to describe Fano factors for CoCu_n clusters on $\text{Cu}(111)$ and will be used here to understand Fano resonances in graphene and why they are different to metals like Cu.

Density of states effects on the Fano factor. Usually, the magnetic orbitals of the ad-atom are strongly localized resulting in $|M_{dt}| \ll |M|$ and consequently

$$q \approx \text{Re } G(E_F) / \text{Im } G(E_F). \quad (11)$$

In a metal with bandwidth D and constant density of states (DOS) in the vicinity of the impurity, $\text{Im } G(\epsilon) = -\pi/2D$ if $-D < \epsilon < D$, we obtain $q \approx -\frac{1}{\pi} \ln \left| \frac{D+E_F}{D-E_F} \right| \approx -\frac{2E_F}{\pi D}$. Hence, $|q| < 1$ and the Kondo effect manifests in STM on normal metals as anti-resonance close to E_F as long as $|M_{dt}| \ll |M|$. This is very different for graphene:

The graphene DOS is $N_0^g(E) = \frac{|E|}{D^2} \cdot \Theta(D - |E|)$ resulting $G(E) = \frac{E}{D^2} \ln \left| \frac{E^2}{D^2 - E^2} \right| - i\pi N_0^g(E)$ and

$$q \approx -\frac{2 \text{sign}(E_F)}{\pi} \ln \left| \frac{E_F}{D} \right|. \quad (12)$$

This results follows directly from linearity of $N(E)$ and the Kramers-Kronig relations. As $D \approx 6 \text{ eV}$ and usually $E_F \lesssim 0.5 \text{ eV}$, the q -factor can be $q \gg 1$ and the Kondo effect may manifest in STM as *resonance* instead of an anti-resonance even for $|M_{dt}| \ll |M|$. This is in contrast to a normal metal, where predominant tunneling into the conduction electron states results in a Kondo-antiresonance in STM. Moreover, Eq. (12) demonstrates that the q -factor in graphene can be expected to depend strongly on the chemical potential.

Energy dependence of the asymmetry factor. Any impurity being coupled to graphene leads to characteristic resonances in the local density of states in the vicinity of the impurity¹⁹ and may consequently alter the Green functions to be inserted into Eq. (11). To understand the role of resonances in the local electronic structure for the q -factor, we illustrate the situation of a realistic impurity by comparing the experimentally important cases of Co on graphene and Co on Cu (111).

For a realistic description of these systems we performed density functional calculations within the generalized gradient approximation (GGA)²⁰ on 6×6 graphene supercells containing one Co ad-atom as well as on $\text{Cu}(111)$ slabs containing 5 Cu layers and one Co ad-atom. The Vienna Ab Initio Simulation Package (VASP)²¹ with the projector augmented wave (PAW)^{22,23} basis sets has been used for solving the resulting Kohn-Sham equations. In this way we obtained relaxed structures for both systems. In particular, we found that GGA predicts Co to sit above the middle of a hexagon on graphene.

To estimate the Fano q -factors we extracted the orbitally resolved Green functions at the impurity site using

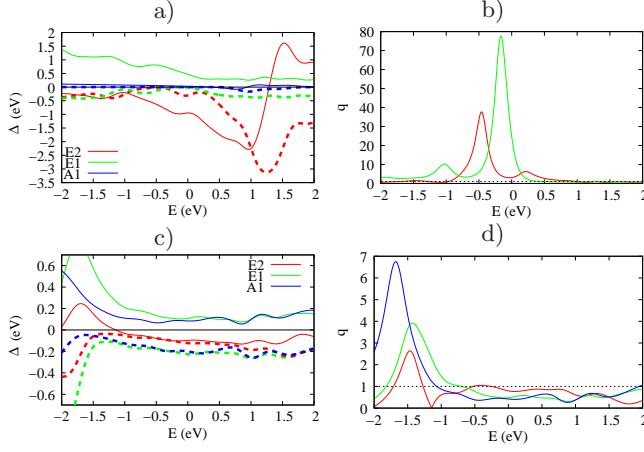


FIG. 1: Hybridization functions Δ (a,c) and calculated asymmetry factors $|q|$ for Co on graphene (upper panel) and Co on Cu (lower panel). For the hybridization functions $\text{Re } \Delta$ is plotted as solid line, $\text{Im } \Delta$ dashed.

atomic orbitals naturally included in the PAW basis sets: The projectors $\langle d_i | \psi_{n\mathbf{k}} \rangle$ of orbitals $|d_i\rangle$ localized at the impurity atoms onto the Bloch eigenstates of the Kohn-Sham problem $|\psi_{n\mathbf{k}}\rangle$ are available when using PAW as implemented in the VASP and these give the local Green functions according to

$$G_{ij}(\epsilon) = \sum_{n\mathbf{k}} \frac{\langle d_i | \psi_{n\mathbf{k}} \rangle \langle \psi_{n\mathbf{k}} | d_j \rangle}{\epsilon + i\delta - \epsilon_{n\mathbf{k}}}. \quad (13)$$

So, we employ here the same representation of localized orbitals as used within the LDA+U-scheme implemented in the VASP-code itself or as discussed in the context of LDA+DMFT in Ref. 24.

The local Green functions at the impurity sites as defined in Eq. (13) are 5×5 matrices which can be used to obtain the hybridization function $\Delta(\epsilon)$ of the impurity:

$$G^{-1}(\epsilon) = \epsilon + i\delta - \Delta(\epsilon). \quad (14)$$

Hence, $\Delta(\epsilon)$ are also 5×5 matrices describing hybridization of 5 d-electrons of Co. In the particular case of Co on Cu(111) and graphene, which are both hexagonal surfaces, these matrices are diagonal and decompose into degenerate blocks of two 2-dimensional and one 1-dimensional representations, transforming under the rotation group C_{6v} as E_1 , E_2 , and A_1 . These components of the hybridization function are depicted in Fig. 1 a and c. At energies close to the Fermi level of graphene all graphene states are in the vicinity of the two Dirac points. These states transform under C_{6v} according to E_1 and E_2 . Hence, the hybridization of the A_1 impurity orbital to the graphene bands is strongly suppressed. Moreover, the crystal field splitting appears to be such that the E_1 orbitals (d_{xz} and d_{yz}) are highest in energy by approx 0.5-1eV as compared to the other d-orbitals. So, the E_1 orbitals are expected to determine the q-factor in STM experiments probing the Kondo effect of Co on graphene.

For Co on graphene Fig. 1 shows that $|\text{Im } \Delta(\epsilon)| \ll |\text{Re } \Delta(\epsilon)|$ in the vicinity of $\epsilon = 0$, which is the Fermi level for undoped graphene. This is very different from the case of Cu, where $|\text{Im } \Delta(\epsilon)|$ and $|\text{Re } \Delta(\epsilon)|$ are mainly on the same order. Using

$$\Delta(\epsilon) = \sum_k \frac{|V_k|^2}{\epsilon + i\delta - \epsilon_k} \quad (15)$$

in combination with Eq. (8) and $|M_{dt}| \ll |M|$ we arrive at

$$q \approx \text{Re } \Delta(E_F) / \text{Im } \Delta(E_F). \quad (16)$$

Within this approximation the projectors and eigenenergies obtained from DFT allow for an ab-initio prediction of q -factors. The Fig. 1 b and d show the q -factors predicted for channels of different C_6 rotational symmetry as calculated for Co on graphene and Cu, respectively, as function of the resonant energy E . $E = 0$ corresponds here to the Fermi level of the undoped system. The calculated q -factors for Co on Cu(111) are typically on the order of $q \lesssim 1$ without pronounced energy dependence. This is in contrast to graphene, where $q > 1$ in a wide energy range and q is strongly energy dependent. So, q is expected to be strongly sensitive to local changes in the chemical potential of graphene, which can be caused by gate voltages, chemical doping or substrate effects. We also point out that this discussion goes well beyond a simple tight binding and linearized dispersion analysis. Presence of defect can substantially change local bands and DOS.

Site dependence of hybridization matrix elements. For Co on graphene, we saw that graphene's Fermi surface being made up by states transforming as E_1 and E_2 under C_6 lead to particular Co orbitals being decoupled from the graphene bands. This special symmetry of graphene's Fermi surface makes the q -factors seen in Kondo resonances in STS particularly dependent of the precise atomic arrangement of the magnetic impurity. This can be illustrated by the site dependence of q -factors for an Anderson impurity sitting, on top of C and on a bridge site in the middle of a hexagon, respectively.

At each adsorption site, a spherically symmetric s-wave impurity can be modelled by equal hopping matrix element V_i to all adjacent sites. For such an Anderson impurity on top of a carbon atom or at a bridge site we obtain

$$V_k = \begin{pmatrix} V_i \\ 0 \end{pmatrix} \text{ and } V_k = \begin{pmatrix} V_i \\ V_i \end{pmatrix}, \quad (17)$$

respectively, by translating that nearest neighbor hopping into the matrix formalism of Eq. (3) and performing the Fourier transformation. Combining this with Eq. (7) results in $B \sim O(E_F)$ for $E_F \rightarrow 0$. This situation corresponds to Eq. 12 with q being enhanced as $E_F \rightarrow 0$.

For the impurity in middle of the hexagon the Fourier transformed hopping reads

$$V_k = \begin{pmatrix} \xi^*(k) \\ \xi(k) \end{pmatrix}. \quad (18)$$

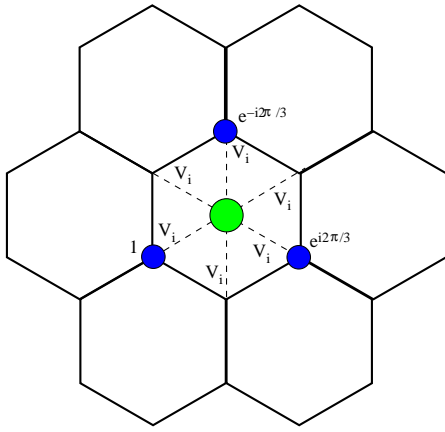


FIG. 2: Model of an Anderson impurity in the middle of the graphene hexagon. Electrons from neighboring can hop onto the impurity by the hopping matrix elements V_i . For an electron from the vicinity of the Brillouin zone corner K phase differences of its wave function at neighboring sites belonging to sublattice A (blue marked atoms) are given. The sum of these phase factors vanishes.

As the dispersion does, this coupling vanishes linearly when approaching the Brillouin zone corners K and K' . As a consequence, any possible Kondo resonance due to such an impurity will lead to $q \gg 1$: Eq. (7) results in $B \sim O(E_F^2)$ for $E_F \rightarrow 0$ in this case — a much stronger enhancement of the q -factor than for the impurity on top of carbon or at a bridge site.

The origin of this effect can be either understood in terms of the C_6 symmetry as discussed above or in terms of destructive quantum interference in graphene lattice: For each state in the vicinity of K (K') the phase of the wave function at neighboring sites of the impurity belonging to one sublattice circulates either clockwise or counterclockwise around the impurity, as illustrated in Fig. 2. The phase of the wave function of atoms in sublattice A having one common nearest neighbor in sublattice B circulates around this atom in sublattice B leading to $\xi(k) \rightarrow 0$ for $k \rightarrow K$ or $k \rightarrow K'$. This cancellation

can also be viewed as a result of Berry phase associated with the Dirac points in pristine graphene. The relation between vanishing of $\xi(k)$ and topological properties of honeycomb lattice was discussed in Ref. 25. Thus, the imaginary part $ImG(E)$ vanishes linearly at the conical point which leads, taking into account analytical properties of $G(E)$ to logarithmic divergence of the q -factor.

In conclusion, we have addressed the Kondo effect in graphene for a realistic d-electron case of Co atom. The crystal field of graphene honeycomb lattice splits the d-orbitals into two doublets, $E_{1,2}$ and one singlet A_1 states. We have performed the first principles calculations and found that E_1 doublet states are responsible for the Kondo effect and for unusual Fano q -factors seen in the experiments¹⁵. For the impurity placed in the middle of hexagon we have found that the same destructive interference that lead to linearly vanishing DOS and to Berry phase is responsible for the anomalously large q -factors in Fano resonance analysis. We thus conclude that nontrivial properties of the Kondo effect in graphene are related to massless Dirac fermion spectrum. The quantum interference effects, like the Fano effect considered here, are extremely sensitive to atomistic details such as specific impurity positions, which can be checked experimentally. Upon completion of this work we learned about the recent preprint by H.-B. Zhuang *et. al.* <http://arxiv.org/abs/0905.4548> that addresses related questions for the case of a s-wave magnetic impurity.

Acknowledgements.

We are grateful to D. Arovas, A. Rosch and J. von Delft for useful discussions. This work was supported by Stichting voor Fundamenteel Onderzoek der Materie (FOM), the Netherlands, by SFB-668(A3), Germany. Work at Los Alamos was supported by US DOE through BES and LDRD funds under the auspices of NNSA of the U.S. Department of Energy under contract No DE-AC52-06NA25396. The work at Stanford University was supported by the Department of Energy, Office of Basic Energy Sciences, Division of Materials Sciences and Engineering, under contract DE-AC02-76SF00515.

* twehling@physnet.uni-hamburg.de

† avb@lanl.gov, <http://theory.lanl.gov>

¹ A. C. Hewson, *The Kondo problem to heavy fermions* (Cambridge University Press, 1993).

² V. Madhavan, W. Chen, T. Jamneala, M. F. Crommie, and N. S. Wingreen, *Science* **280**, 567 (1998), <http://www.sciencemag.org/cgi/reprint/280/5363/567.pdf>, URL <http://www.sciencemag.org/cgi/content/abstract/280/5363/567>.

³ N. Knorr, M. A. Schneider, L. Diekhöner, P. Wahl, and K. Kern, *Phys. Rev. Lett.* **88**, 096804 (2002).

⁴ L. Limot and R. Berndt, *Appl. Surf. Science* **237**, 572 (2004).

⁵ N. Néel, J. Kröger, R. Berndt, T. O. Wehling, A. I. Lichten-

stein, and M. I. Katsnelson, *Phys. Rev. Lett.* **101**, 266803 (pages 4) (2008), URL <http://link.aps.org/abstract/PRL/v101/e266803>.

⁶ K. S. Novoselov, A. K. Geim, S. V. Morozov, D. Jiang, Y. Zhang, S. V. Dubonos, I. V. Grigorieva, and A. A. Firsov, *Science* **306**, 666 (2004).

⁷ K. S. Novoselov, A. K. Geim, S. V. Morozov, D. Jiang, M. I. Katsnelson, I. V. Grigorieva, S. V. Dubonos, and A. A. Firsov, *Nature* **438**, 197 (2005).

⁸ Y. Zhang, Y.-W. Tan, H. L. Stormer, and P. Kim, *Nature* **438**, 201 (2005).

⁹ C. R. Cassanello and E. Fradkin, *Phys. Rev. B* **53**, 15079 (1996).

¹⁰ K. Sengupta and G. Baskaran, *Physical Review B (Con-*

- densed Matter and Materials Physics) **77**, 045417 (pages 5) (2008), URL <http://link.aps.org/abstract/PRB/v77/e045417>.
- ¹¹ G. U. P. S. Cornaglia and C. A. Balseiro, Phys. Rev. Lett. **102**, 046801 (2009).
 - ¹² A. V. Balatsky, I. Vekhter, and J.-X. Zhu, Rev. Mod. Phys. **78**, 373 (2006).
 - ¹³ F. Schedin, A. K. Geim, S. V. Morozov, E. W. Hill, P. Blake, M. I. Katsnelson, and K. S. Novoselov, Nat. Mater. **6**, 652 (2007).
 - ¹⁴ T. O. Wehling, K. S. Novoselov, S. V. Morozov, E. E. Vdovin, M. I. Katsnelson, A. K. Geim, and A. I. Lichtenstein, Nano Lett. **8**, 173 (2008).
 - ¹⁵ H. Manoharan et al., to be published.
 - ¹⁶ P. R. Wallace, Phys. Rev. **71**, 622 (1947).
 - ¹⁷ G. W. Semenoff, Phys. Rev. Lett. **53**, 2449 (1984).
 - ¹⁸ V. Madhavan, W. Chen, T. Jamneala, M. F. Crommie, and N. S. Wingreen, Phys. Rev. B **64**, 165412 (2001).
 - ¹⁹ T. O. Wehling, A. V. Balatsky, M. I. Katsnelson, A. I. Lichtenstein, K. Scharnberg, and R. Wiesendanger, Phys. Rev. B **75**, 125425 (2007).
 - ²⁰ J. P. Perdew et al., Phys. Rev. B **46**, 6671 (1992).
 - ²¹ G. Kresse and J. Hafner, J. Phys.: Condes. Matter **6**, 8245 (1994).
 - ²² P. E. Blöchl, Phys. Rev. B **50**, 17953 (1994).
 - ²³ G. Kresse and D. Joubert, Phys. Rev. B **59**, 1758 (1999).
 - ²⁴ B. Amadon, F. Lechermann, A. Georges, F. Jollet, T. O. Wehling, and A. I. Lichtenstein, Phys. Rev. B **77**, 205112 (pages 13) (2008), URL <http://link.aps.org/abstract/PRB/v77/e205112>.
 - ²⁵ F. G. J. L. Mañes and M. A. Vozmediano, Phys. Rev. B **75** (2007).